Two New Triple Star Systems with Detectable Inner Orbital Motions and Speckle Interferometry of 40 Other Double Stars

Russell Genet[1,2,3,4], Henry Zirm[5], Francisco Rica[6], Joseph Richards[3], David Rowe[7], and Daniel Gray[8]

1. California Polytechnic State University, San Luis Obispo
2. Concordia University, Irvine, California
3. Cuesta College, San Luis Obispo, California
4. University of North Dakota, Grand Forks
5. Markt Schwaben, Germany
6. Agrupación Astronómica de Mérida, Mérida (Badajoz), Spain
7. PlaneWave Instruments, Rancho Dominguez, California
8. Sidereal Technology, Portland, Oregon

Abstract Speckle interferometry observations of 42 double stars with a separation between 0.5″and 2.0″ were made at Pinto Valley Observatory with a 0.5-meter PlaneWave Instruments CDK20 telescope equipped with a portable Andor Luca-S EMCCD-based speckle camera. STF162 AB / CHR4 Aa, Ab and STF 425, both without previously published orbits, were found to be triple systems. We provide orbits of the inner pairs.

Introduction

Observations were made of 42 relatively close (0.4 to 2.5 arcseconds) double stars. Two were found to be triple systems, and we provide orbits for the inner pairs of these newly discovered systems. Of the remaining 41 doubles, 18 were known binaries with published orbits, while the remaining 19 doubles were without published orbits and many were probably just optical doubles.

All observations were made with a portable speckle camera system that featured an Andor Luca-S EMCCD camera, which has 10 µ square pixels in a 658x496 pixel array, and x8 magnification (Genet 2013). All integrations were 15 ms in length taken through a Johnson V filter. Observations were made with 1x1 binning and 128x128 Regions of Interest (RoIs) that were read out in the "Kinetic" frame-transfer mode at approximately 67 frames/second.

The camera was mounted on a 0.5-meter PlaneWave Instruments CDK20 corrected Dall-Kirkham Cassegrain telescope equipped with a Sidereal Technology (SiTech) Servo Controller and high-resolution, on-axis encoders. This telescope is located at David Rowe's Pinto Valley Observatory located in the heart of the Mojave National Preserve in Southern California.

Calibration

By observing binaries in the Sixth Catalog of Orbits of Visual Stars (Hartkopf & Mason 2012), 17 independent estimates were obtained of the camera angle and pixel scale. For the night of observation, the predicted separations and position angles were calculated based on the ephemerides in the catalog. These values were used as inputs to the double star reduction program REDUC (Losse 2012) in its "Calibration" (as opposed to "Measure") mode, to determine the camera's position angle and pixel scale via "Autocorrelation" (Figure 1).

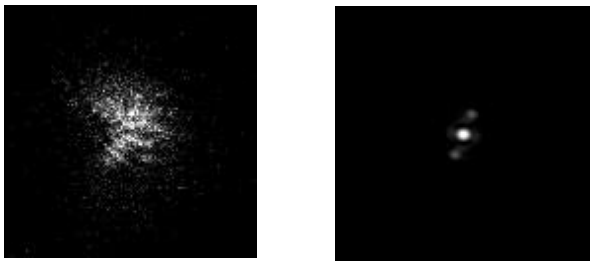

Figure 1. Typical single speckle image (left) and autocorellogram (right). These were for STT20, a binary with a separation of 0.584″. Integration times for 2000 frames were 15 ms with a Johnson V filter.

Calibration results from 17 binaries are summarized in Table 1. The camera angle is in degrees from north, while the pixel scale is in arcseconds/pixel with 10 micron pixels. The negative camera angle is a rotation west of north, i.e., 337.54°. Variances include both measurement errors and discrepancies between the predicted and actual (but unknown) true values.

	Camera Angle	Pixel Scale
Mean	-22.46	0.0538
Standard Deviation	1.54	0.0020
Standard Error of the Mean	0.37	0.0005

Table 1. Calibration results from 17 binaries.

Five east-west drifts of two relatively bright stars, 58 And and psi Per, were obtained. "Synthesis Drift" in REDUC performed the analysis by fitting linear least squares lines through the centroids to provide the camera angles, with results shown in Table 2. The standard errors of the mean are just indicators of internal precision within the repeated drift runs on each star. If measurements for 17 different single drift stars had been obtained, as was the case for 17 different binaries, then it could have been determined if there were systematic differences between various drifts. With only two drift stars, however, there was no way to reliably estimate the magnitude of any such systematic errors.

Camera Angle (°)	58 And	psi Per
Mean	-23.13	-22.9
Standard Deviation	1.04	0.71
Standard Error of the Mean	0.47	0.35

Table 2. Camera angle from five drift stars.

Drifts, with their larger internal errors and unknown external errors, were not used in the final calibration. Total reliance was placed on the mean camera angle and pixel scale derived from 17 binaries with known orbits. These values and their standard errors of the mean were, respectively, -22.46 ± 0.37° and 0.0538 ± 0.0005 ″/pixel.

Repeatability and Accuracy

Once the camera angle and pixel scale were derived, an estimate was made of the internal precision (i.e., internal consistency) and external (overall) error of the observations, using 18 binaries that were in the *Sixth Catalog of Orbits of Visual Stars* (Hartkopf & Mason 2012).

Each observation, which consisted of 2000 frames (each with 15 ms integration), was recorded as a data cube. Each cube was then broken up into four sub-cubes of 500 frames each, providing four samples that allowed an average solution to be calculated together with its corresponding standard error of the mean. Admittedly a sample of only four is small, but even a rough estimate of internal precision (repeatability) can be useful.

There is, of course, a degree of circularity in using the same set of binaries to not only determine the camera angle and pixel scale, but to also make an accuracy estimate (regression toward the mean). Thus the accuracy estimate may be an underestimate (Mendenhall et al. 1990). On the other hand, since the accuracy estimate includes both observational errors and errors in the orbital position predictions, it may be an over-estimate. It should also be noted that all observations were made within a single night, thus night-to-night variances are not represented.

Table 3 summarizes the results of the internal precision and external accuracy analysis. All values are in milli-arcseconds (mas). The values for the position angle, θ, are the "rotational" error distances in mas. The conversion of the position angle errors to tangential distance errors (simply the product of θ and ρ) allowed them to be compared on a one-to-one basis with the separation errors. At its heart, double star astrometry is the determination of the positions of centroids in an x/y plane.

	Precision	Accuracy
θ	1.1	16.0
ρ	3.4	24.8
RSS	3.6	29.5

Table 3. Internal precision and external accuracy estimates in milli arcseconds (mas).

The internal precision errors were less than the external accuracy errors by a factor of eight. It might be noted that, if instead of considering the variance within single data cubes, precision had been estimated by comparing the repeatability of observations of the same binaries across several nights (not possible in our one-night run), the internal precision would have been somewhat poorer and thus there would not have been as large a difference between internal precision and external accuracy. Also, if only binaries with high grade orbits had been used, the accuracy would have been better, further reducing the difference. The θ and ρ errors were root-sum-squared together for final, single error values for internal precision and external errors, as shown in Table 3. Thus the overall estimate of accuracy for this run was about 30 mas.

Observational Results

Observations were made over four hours on the evening of November 19, 2012, with a midpoint of almost exactly 21:00 Pacific Standard Time (UT+8). This corresponds to 07:00 UT November 20, 2012, to JD 2456251.792, and to the Besselian epoch of 2012.8880. All observations were made through a Johnson V filter with 15 ms integrations. The electron-multiplying gain was adjusted to roughly half well (half full scale) or, where that could not be reached, set at near maximum gain.

Each double star took four minutes, on average, to observe. With 15 ms integration time for each of 2000 frames in a data cube and the camera operating in the frame transfer mode, each observation took about 30 seconds. Thus the duty cycle was about 12.5%. The remaining 210 seconds were used to look up the next double to observe, command the telescope to go to that double, slew to the double, acquire the double (often using a spiral search routine written on the spot by Gray), roughly center the double on the camera display with the telescope controls, move (with the mouse) the Region of Interest (RoI) over the double, set the camera's electron-multiplying gain, check to make sure everything was okay, and, finally, start the integration.

Observational results are provided in Table 4. A Johnson V filter (540 nm center wavelength, 90 nm FWHM) was used for all observations. The first four columns (WDS Designation, Discoverer Designation, Primary Magnitude, and Secondary Magnitude) were copied straight from the Washington Double Star Catalog (Mason et al. 2013). The fifth column is the Besselian epoch. The measured values for θ and ρ (observational epoch) were determined with REDUC in the "Measure" mode, using the camera angle (Δ) and pixel scale (E) from the calibration discussed above as inputs.

WDS Designation	Discoverer	Primary	Secondary	Date	θ	ρ	O-C	O-C	Orbit	Orbit	Note
α, β (2000)	Designation	Magnitude	Magnitude	Besselian	(°)	(")	(θ)	(ρ)	Grade	Reference	
00063+5826	STF 3062	6.42	7.32	2012.8876	352.8	1.521	0.6	-0.031	2	Kiyaeva et al. (2001)	
00546+1911	STT 20AB	6.12	7.19	2012.8876	179.5	0.584	0.2	0.016	3	Docobo & Ling (2007)	
00550+2338	STF 73AB	6.12	6.54	2012.8876	326.7	1.067	0.1	-0.024	2	Muterspaught et al. (2010)	
01095+4715	STT 515AB	4.59	5.61	2012.8877	118.2	0.495	0.1	-0.022	4	Muterspaught et al. (2010)	
01097+2348	BU 303	7.32	7.56	2012.8877	292.5	0.603					
01106+5101	BU 235AB	7.54	7.82	2012.8877	139.0	0.827	1.8	-0.028	4	Seymour et al. (2002)	
01283+4247	AC 14	8.29	8.88	2012.8878	91.9	0.765					
01401+3858	STF 141	8.28	8.61	2012.8878	303.4	1.666					
01493+4754	STF 162AB	6.47	7.22	2012.8877	198.8	1.946	0.5	-0.017	L+9	Genet et al. (this work)	b
01532+1526	BU 260	8.75	8.97	2012.8878	259.6	1.120	-0.7	0.027	5	Cvetkovic & Novakovic (2006)	
02062+2507	STF 212	8.35	8.71	2012.8878	161.8	1.904					
02140+4729	STF 228	6.56	7.21	2012.8877	295.6	0.749	0.0	-0.015	2	Soderhjelm (1999)	
02331+5828	STF 272	8.33	8.36	2012.8880	216.9	1.911					
02388+3325	STF 285	7.48	8.14	2012.8880	162.7	1.708					
02422+4242	STT 44AB	8.46	8.96	2012.8880	55.9	1.387					
02529+5300	STF 314AB,C	6.95	7.26	2012.8879	315.7	1.549					
02589+2137	BU 525	7.47	7.45	2012.8879	272.4	0.537	-2.1	0.043	4	Costa (1978)	
02592+2120	STF 333AB	5.17	5.57	2012.8879	209.9	1.381	0.4	0.025	4	Rica et al. (2012)	
03054+2515	STF 346AB	6.21	6,19	2012.8879	254.1	0.421	-3.2	-0.055	3	Heintz (1997)	
03058+4342	BU 1175	7.23	8.80	2012.8879	273.3	0.683					
03177+3838	STT 53	7.73	8.50	2012.8880	237.1	0.617	-1.0	0.016	3	Alzner (1988)	
03233+2058	STF 381	7.56	8.75	2012.8880	107.9	1.056					
03250+4013	HU 1058	8.22	8.83	2012.8880	113.8	0.840					
03285+5954	STF 384AB	8.13	8.85	2012.8880	272.4	1.953					
03302+5922	STF 389AB	6.42	7.89	2012.8879	71.5	2.523					
03312+1947	STF 403	8.71	8.92	2012.8880	172.3	2.290					
03344+2428	STF 412AB	6.60	6.86	2012.8879	353.1	0.742	0.8	0.001	3	Scardia et al. (2002)	
03401+3407	STF 425	7.52	7.60	2012.8879	60.8	1.898	0.7	-0.020	L+9	Genet et al. (this work)	b
03407+4601	STT 59	7.90	8.85	2012.8880	355.6	2.819					
03454+4952	HU 103AB	8.70	8.86	2012.8879	202.2	1.158					
04064+4325	A 1710	8.16	8.27	2012.8879	311.9	0.618	1.5	-0.001	3	Heintz (1982)	
04069+3327	STT 71AB	6.86	8.66	2012.8879	229.2	0.743					
04182+2248	STF 520	8.26	8.46	2012.8880	78.8	0.632	-2.5	0.039	3	Hartkopf & Mason (2001)	
04227+1503	STT 82AB	7.31	8.63	2012.8880	332.6	1.210	-1.2	-0.017	3	Mason et al. (2004)	
04233+1123	STF 535	6.95	8.29	2012.8878	270.5	1.054	0.8	0.002	5	Hartkopf & Mason (2000)	
04422+3731	STF 577	8.38	8.45	2012.8880	337.5	0.723				Mason et al. (2004)	
04478+5318	HU 612	7.06	8.54	2012.8880	0.3	0.699	-0.4	0.030	5	Novakovic (2007)	
05055+1948	STT 95	7.02	7.56	2012.8880	296.4	0.926	-0.6	-0.033	4	Jasinta (1996)	
05103+3718	STF 644AB	6.96	6.78	2012.8880	222.6	1.647					
05167+1826	STF 670AB	7.72	8.28	2012.8880	165.1	2.520					
05188+5250	STF 657	8.30	8.81	2012.8880	310.5	0.952					
05240+2458	STF 694AB	8.65	8.54	2012.8880	14.2	1.379					

Table 4. Double star speckle measures.

Notes:
[a] In close agreement with recent speckle observations in θ, but off in ρ. See orbital plot below.
[b] Our analysis suggests this is a gravitationally bound triple system.
[c] Similar to "a" above, in close agreement in ρ, but other θ speckle observations were about 242°.
[d] Significant trend in past speckle interferometry observations confirmed by our observation.
[e] As above, significant trend confirmed by our observation.

The observed minus calculated (O-C) values for θ and ρ were calculated by comparing observed values with those interpolated from the Sixth Catalog of Orbits of Visual Stars ephemerides to the night of observation.

Two New Triple Star Systems with Detectable Inner Orbital Motions

Table 5 provides fundamental information on the two systems we suspected to be triple star systems. We found that the superimposed movements are clearly reflected in the measurements, especially in the position angles, so we calculated the orbital elements for the inner systems. We did not calculate orbits for the presumably very long period outer systems, simply assuming that their path over a short time scale was linear. Meaningful orbital calculations of the outer pairs may only be possible after further measurements from coming decades. Lists of measurements and resulting residuals used can be obtained by request.

Washington Double Star catalogue	WDS 01493+4754	WDS 03401+3407
Discoverer Designation	STF162 AB | CHR 4 Aa,Ab	STF 425
Aitkens Double Star catalogue Nr.	ADS 1438	ADS 2668
Henry Draper catalogue Nr.	HD 11031	HD 22692
Hipparcos catalogue Nr.	HIP 8475	HIP 17129
Coordinates α_{2000} / δ_{2000}	27.°31 / +47.°90	55.°03 / +34.°12
Parallax (van Leeuwen 2007)	0.”00784 ± 0.”00102	0.”02173 ± 0.”00084
Distance to Sun (in Parsecs)	$127.6^{+19.0}_{-14.7}$	$46.0^{+1.9}_{-1.7}$
Combined visual magnitude (V in mag)	5.82	6.82
Differential visual magnitude (dV in mag)	0.8 | $\sim 3_{\text{estimated}}$	0.1
Combined spectral and luminosity class	A3V	F9 V

Table 5. Designations, coordinates, and other properties.

WDS 01493+4754 = STF162 AB / CHR4 Aa,Ab = ADS 1438

Located in Perseus, this system is at least triple. The notes entry for this system in the Washington Double Star Catalog contains the following information: “Although this new component is indicated as Aa,Ab, we have not firmly established whether it is associated with the A or B component of the wide pair. B is a spectroscopic binary. The system appears to be quintuple” (McAlister et al. 1987).

We considered whether the combined and overlaid movement sequences (the three proven components) are visible and predictable. For the inner pair CHR4 Aa,Ab measurements exist from 1984 to 1994. These cover an arc of about 60 degrees and show a well-defined orbital arc. After 1994, the inner system unfortunately could not be resolved. But this suborbital motion is detectable in the residuals of the outer system STF162 AB (Figure 2), so we determined a provisional period of the internal system. The measurements for STF162 AB covers nearly 180 years; the first successful separation of the main components are from J.F.W. Hershel in 1828.

We began our analysis with a weighted fit, calculating only the linear motion parameters in Cartesian coordinates. The general form was adopted from Debehogne and de Freitas Mourao (1977). The resulting residuals (in arcseconds) are plotted against time as shown in Figure 2.

Clearly visible is the expected “wobble”, induced by the overlaid motion of the inner pair CHR4 Aa,Ab. A first tentative period of nearly 35 years was assumed from the residuals in Figure 2. A first combined differential correction fit with zero eccentricity and the preliminary period was made. The resulting period for CHR4 Aa,Ab is P_{inner} = 36.9 years with an uncertainty of ±0.6 years. The other tentative (circular) elements are T_{inner} = 2004.6, α_{inner} = 0.056 arcseconds and a node of $\Omega_{2000\ inner}$ = 16 degrees. With these tentative elements it is possible to calculate an independent visual orbit for the inner pair based on the available speckle measurements for CHR4 Aa,Ab. A differential correction routine in rectangular coordinates was used (van den Bos 1926, also see Heintz 1978). On this basis, the correction factors for the elements ΔT_{inner}, Δe_{inner}, ΔA_{inner}, ΔB_{inner}, ΔF_{inner} and ΔG_{inner} are calculated. The period was assumed to be known (P_{inner}=36.9 years), thus fixed and not corrected. After several iterations, a new independent visual orbit for the inner pair was found (Table 6). Subsequently, the linear path and the inner photo centric semi-major axis based on the new visual orbits were calculated, based on the combination of differential correction for linear and orbital motion in rectangular coordinates. All final elements are collected in Table 6. The ephemerides for the inner and outer components are collected in Table 7. Additional figures for the final outer combined linear and photo centric solution and the inner visual orbital solution can be found in Figures 3 and 4.

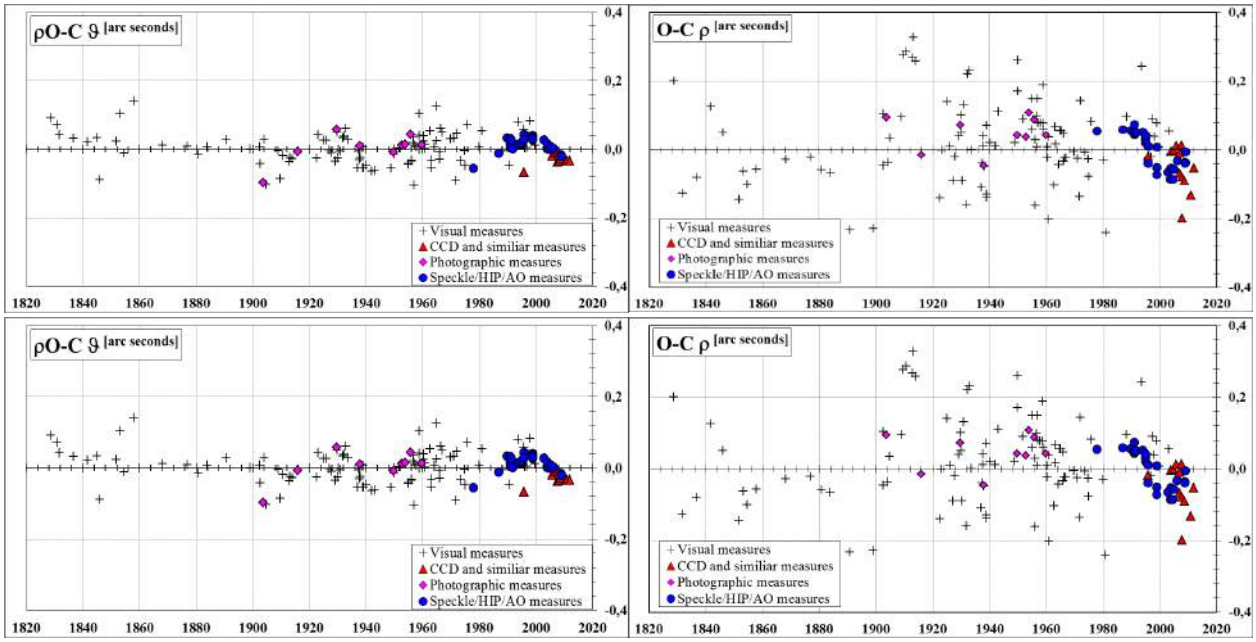

Figure 2. Residual plots for STF 162 AB, only linear motion assumed.

linear solution main components (outer)				new visual orbit (inner) with photo centric amplitude, calculated from linear motion residuals from STF 162 AB			
$X_0 = \Delta\delta$	-1.663	± 0.029	arcseconds	P_{inner}	36.9	± 0.6 (adopted, see text)	years
$\mu_X = \mu_\delta$	-0.00241	± 0.00015	arcseconds / year	T_{inner}	2004.8	± 3.8	years
$Y_0 = \Delta\alpha_{cos\delta}$	-0.957	± 0.050	arcseconds	e_{inner}	0.234	± 0.069	-
$\mu_Y = \mu_{\alpha cos\delta}$	0.00418	± 0.00012	arcseconds / year	α_{inner}	0.040	± 0.003	arcseconds
t_0	1937.8	± 12.5	years	a_{inner}	0.122	± 0.027	arcseconds
ϑ_0	209.9	± 1.7	degrees	i_{inner}	34.4	± 15.5	degrees
ρ_0	1.919	± 0.004	arcseconds	$\omega_{secondary\ inner}$	348.6	± 43.8	degrees
μ_{XY}	0.00482	± 0.00019	arcseconds / year	$\Omega_{2000\ inner}$	32.0	± 40.5	degrees

Table 6. Final combined linear + orbital results for STF 162 AB and CHR 4 Aa,Ab.

The mass sum for the innerpair CHR 4 Aa,Ab is $\Sigma M = 2.8 \pm 1.2\ M_{Sol}$, the errors in mass resulting from orbit and parallax uncertainties. With the relation from Equation 1, it is not possible to estimate the individual masses for the single members of CHR 4 Aa,Ab. The value f-β=0.33 ± 0.03 was obtained. However, since the difference in brightness is not known (no measurements are available), a preliminary estimate must be made. A luminosity ratio β can be calculated if we estimate a tentative assumed brightness difference dV. If dV = 3 ± 1 mag assumed, a mass ratio f = 0.39 ± 0.06 was calculated. This results in individual masses for $Mass_{CHR\ 4\ Aa} = 1.7 \pm 0.8\ M_{Sol}$ and for $Mass_{CHR\ 4\ Ab} = 1.1 \pm 0.5\ M_{Sol}$.

Ephemerides	Combined motion		Linear path only		Photo centric orbit only		Visual orbit inner pair CHR 4 Aa,Ab	
	ϑ_{2000} [°]	ρ ["]	ϑ_{2000} [°]	ρ ["]	Δδ ["]	Δα ["]	ϑ_{2000} [°]	ρ ["]
2013.0	198.3	1.964	199.2	1.953	-0.021	0.026	128.6	0.103
2015.0	198.1	1.979	198.9	1.955	-0.032	0.019	148.7	0.114
2017.0	198.0	1.991	198.7	1.957	-0.040	0.011	165.1	0.126
2019.0	198.0	2.001	198.4	1.958	-0.045	0.001	178.7	0.137
2021.0	197.9	2.008	198.1	1.960	-0.047	-0.009	190.5	0.145
2025.0	197.9	2.012	197.6	1.964	-0.042	-0.026	211.6	0.150
2030.0	197.7	2.001	196.9	1.970	-0.022	-0.038	240.2	0.132
2035.0	197.1	1.976	196.2	1.975	0.009	-0.031	285.7	0.097
2040.0	195.8	1.953	195.5	1.981	0.029	-0.001	358.7	0.089

Table 7. Ephemerides for STF 162 AB and CHR 4 Aa,Ab.

These mass values are only preliminary, but they could help determine the parameters of the individual components. It is important to obtain new and accurate measurements of the positions and brightness differences of the inner components. By using lucky imaging, it may be possible to determine the assignment of the inner system to STF 162 A or STF 162 B.

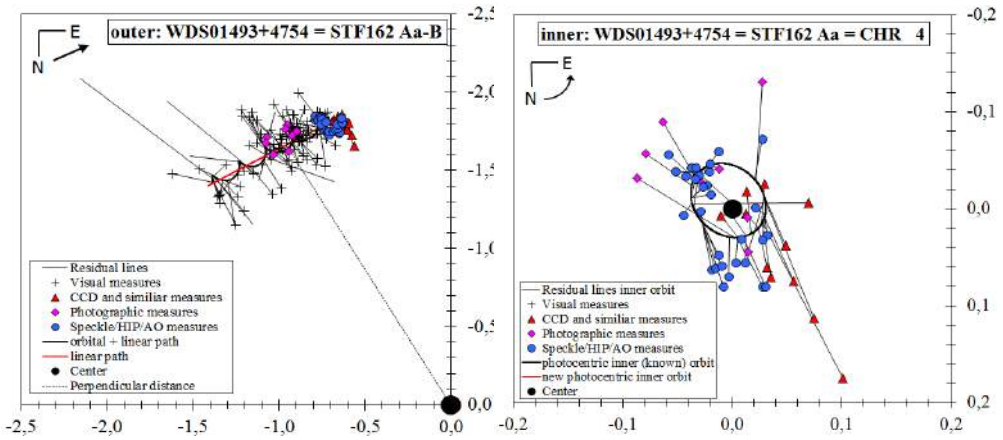

Figure 3. Outer combined Linear + orbital solution (left), and inner photo centric orbital solution only, visual measures not shown (right).

WDS 03401+3407 = STF 425 = ADS 2668

The double star STF 425, located in constellation Perseus, was first discovered by William Herschel in 1783. However, he only measured the position angle. Only 40 years later, J. South obtained the first complete measurement. The two main visible stars currently have a separation of about 2 arcseconds. These stars have almost the same brightness and are yellow main sequence stars with the common spectral class F9. Basic information on STF 425 is provided above in Table 5. Rica noted that STF 425 shows an interesting trend as can be seen in Figure 6. A preliminary Cartesian plot of the secondary's x and y positions showed an "S" shaped wobble, suggesting a triple system. The speckle interferometry observations prior to ours were made by McAlister et al. (1987), Scardia et al. (2007), Prieur et al. (2008), Castets and Tregon (2009), Scardia et al. (2011), and Mason et al. (2012b). Past observations for the analysis were supplied by the US Naval Observatory to which we added our recent speckle observation.

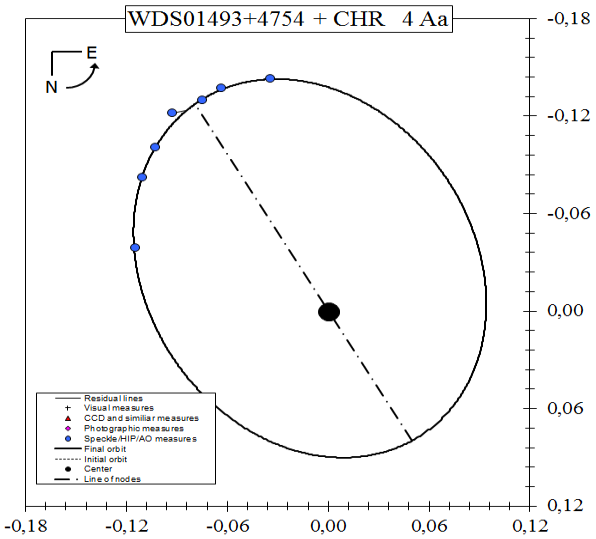

Figure 4. Inner visual orbital solution for CHR 4 Aa,Ab.

Andre Tokovinin pointed out to us that STF 425 was observed in 2012 with Robo-AO on the 1.5-meter telescope at Palomar Observatory, and he saw no companion around A or B.

We initiated our analysis with a weighted fit, calculating only linear motion parameters in Cartesian coordinates. The general form was adopted from Debehogne and de Freitas Mourao (1977). The resulting residuals (in arcseconds) are plotted against time and shown in Figure 5.

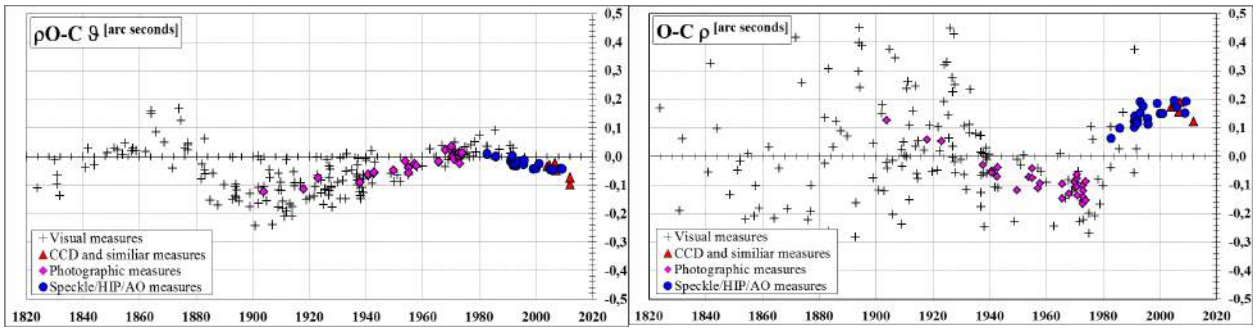

Figure 5. Trend plots for STF 425, only linear motion assumed.

Clearly visible in the position angle (θ) and separation (ρ) rho residuals in Figure 5, based on a preliminary linear fit, is remarkable "wobble" of about 0.1 arcseconds. This is a very clear indication of a suborbital movement caused by a possible invisible companion. We performed a combined calculation of the linear (for the outer orbit) and the orbital (for the inner orbit) movement in Cartesian coordinates, based on the combination of differential correction for 7 orbital elements (van den Bos, 1926) and the 4 parameters from linear motion (see above).

This differential correction fit was made based on the first linear elements and an assumed fixed period of ~110 years. For simplification, zero eccentricity was assumed, and thus only A_{inner}, B_{inner}, F_{inner}, G_{inner} and the four linear elements had to be calculated.

Subsequently, we applied a reweighting procedure as described by Irwin, Walker, and Young (1996). A combined linear and orbital fit based on the initial outer (linear) and inner (orbital) fit was made by freeing the correction parameters for eccentricity and periastron passage, with final results as shown in Table 8.

We did not assume that only orbital motion was detectable in the inner pair. We performed a combined orbital-orbital solution (for both the outer and inner orbits) in Cartesian coordinates (with maximum 14 possible unknowns) following van den Bos (1926). The final weights from the linear and orbital fits were used. For the outer orbit, zero eccentricity was assumed, thus differential corrections were only for A $_{outer}$, B $_{outer}$, F $_{outer}$, G $_{outer}$ and a period fixed with a preliminary period of P outer = 2000 years. The inner orbit was, at first, adopted from a linear orbital solution and was not differential corrected at first. But it turned out that the orbit calculation is only possible if the period is fixed and the orbit is assumed at circular. Thus differential corrections were performable only for A_{outer}, B_{outer}, F_{outer}, G_{outer}. In this case, different fixed periods can be calculated for an orbit, but it is clear that an orbital curvature was barely recognizable and therefore a simplistic circular orbit calculation was vague. Thus the preferred solution is the linear + orbital solution, provided in Table 8.

Linear solution main components (outer)				New photo centric orbit (inner)			
$X_0 = \Delta\delta$	1.141	± 0.021	arcseconds	P_{inner}	106.5	± 1.7	years
$\mu_X = \mu_\delta$	0.00933	± 0.00011	arcseconds / year	T_{inner}	1980.19	± 0.94	years
$Y_0 = \Delta\alpha_{cos\delta}$	1.287	± 0.019	arcseconds	e_{inner}	0.612	± 0.050	-
$\mu_Y = \mu_{\alpha cos\delta}$	-0.00827	± 0.00025	arcseconds / year	α_{inner}	0.179	± 0.008	arcseconds
t_0	2045.3	± 2.6	years	i_{inner}	106.8	± 2.4	degrees
ϑ_0	48.4	± 0.9	degrees	$\omega_{1\ inner}$	77.8	± 3.4	degrees
ρ_0	1.719	± 0.006	arcseconds	$\Omega_{2000\ inner}$	65.5	± 2.6	degrees
μ_{XY}	0.01247	± 0.00027	arcseconds / year				

Table 8. Final combined linear + orbital results for STF 425.

The final linear + orbital fit produces residuals with rms and MA values in position angle (θ) of 0.50/0.32 degrees, the rms/MA values in separation (ρ) are 0.043 and 0.026 arcseconds. The ephemerides up to 2040 are shown in Table 9.

Ephemerides	Combined motion		Linear path only		Photo centric orbit only		Estimated visual orbit inner pair a = 0.59 arcseconds assumed	
	ϑ_{2000} [°]	ρ ["]	ϑ_{2000} [°]	ρ ["]	Δδ ["]	Δα ["]	ϑ_{2000} [°]	ρ ["]
2013.0	60.1	1.918	61.6	1.766	0.117	0.109	223.0	0.520
2015.0	59.3	1.907	60.8	1.760	0.117	0.102	221.0	0.506
2017.0	58.4	1.896	60.0	1.755	0.117	0.094	218.9	0.490
2019.0	57.5	1.885	59.2	1.750	0.116	0.086	216.6	0.473
2021.0	56.7	1.874	58.4	1.746	0.115	0.078	214.1	0.454
2025.0	54.9	1.851	56.8	1.738	0.112	0.061	208.5	0.415
2030.0	52.8	1.823	54.8	1.730	0.106	0.038	199.9	0.366
2035.0	50.5	1.796	52.7	1.724	0.097	0.015	188.5	0.319
2040.0	48.3	1.770	50.6	1.721	0.086	-0.009	173.8	0.283

Table 9. Ephemerides for STF 425 to 2040.

Although it was not possible to assign the movement of the invisible companion to either component A or B, for simplification we assigned it tentatively to component A. If it is detectable, only further observations are likely to provide the assignment of the invisible companion to the appropriate component. The apparent motion of the linear and orbital paths, the measurements, and the corresponding residual lines are displayed in Figure 6; the axis units are in arcseconds.

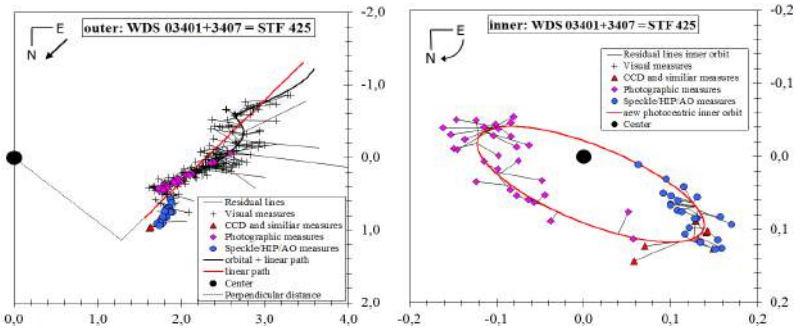

Figure 6. Outer combined Linear + orbital solution (left), and inner photo centric orbital solution only, visual measures are not shown (right).

Summarizing, the inner orbit has a period of about 107 years. The eccentricity seems to be large (e~0.6) and the photo centric half axis is $\alpha = 0.18$ arcseconds. Both visible members of this system are nearly equal in brightness, color, and absolute magnitude. Thus it can be assumed that each component is a late F main sequence star with a mass of M_{SOL} ~1.2 (Schmidt-Kaler, 1982). With this result, one can try to estimate the mass of the invisible companion. For this estimate we need some formulas, described below.

To determine the total mass (ΣM) of a visual binary system, the period (P in years), the great semi major axis (a in arcseconds), and the parallax (π in arcseconds) are required, given in Equation 1.

$$\Sigma M = M_{VC} + M_{IC} = a^3 \cdot \pi^{-3} \cdot P^{-2} \qquad \textit{Eq. 1}$$

The total mass (ΣM) of the sub system is composed by the mass one of the visible component (M_{VC} in units of Sol mass) and the mass of the invisible component (M_{IC} in units of Sol mass). Further, we require an estimate of the mass ratio (B). In the present case, this is simply taken as the ratio of the photo centric semi major axis (α in arcseconds) of the visible component to the semi major axis (a in arcseconds) of the orbital path of the both components:

$$B = \frac{\alpha}{a} = \frac{M_{IC}}{M_{VC} + M_{IC}} \qquad \textit{Eq. 2}$$

The reorganization and combination of Equation 1 and Equation 2 leads to the following relations:

$$\alpha \cdot \frac{M_{VC} + M_{IC}}{M_{IC}} = \alpha \cdot \frac{a^3 \cdot \pi^{-3} \cdot P^{-2}}{M_{IC}} = a = \left[\left(M_{VC} + M_{IC} \right) \cdot \pi^3 \cdot P^2 \right]^{1/3} \qquad \textit{Eq. 3}$$

As a result we only have two unknowns; the mass of the invisible component (M_{IC}) and the semi major axis a. The mass of the visible component (M_{VC}) we can adapt from Schmidt-Kaler (1982) tables for physical parameters of main sequence stars. Within reasonable limits we estimate a theoretical value for the mass of the invisible companion.

With Equation 4 we can derive the theoretical (visible) half axis of the inner orbit and the theoretical mass of the visible primary iteratively, until this value is the same as the initial mass for an late F type main sequence star: $M_{VC} = 1.2\ M_{SOL}$.

$$M_{VC} = \frac{M_{IC}}{\alpha} \left[\left(M_{VC} + M_{IC} \right) \cdot \pi^3 \cdot P^2 \right]^{1/3} - M_{IC} \qquad \textit{Eq. 4}$$

If the calculated mass value coincides with the theoretical value, the value of the visual semi major axis (a in arcseconds) can be calculated via:

$$a = \left[\left(M_{VC} + M_{IC} \right) \cdot \pi^3 \cdot P^2 \right]^{1/3} \qquad \textit{Eq. 5}$$

The calculated value for the photo centric half axis, is α_{calc} = 0.18 arcseconds. If the Mass for the invisible companion matches with 1.2 M_{SOL}, then we obtain the result of 0.53 M_{SOL} for the invisible companion. The theoretical, visible half axis is ~ a_{inner} = 0.586 arcseconds. A star with a mass of 0.5 M_{SOL} is possible for an early M dwarf star, with a corresponding large difference in brightness. This may be the reason that this companion is not resolvable in visual pass bands.

Comparison with Previous Observations

To compare the 20 binaries observed with all previously reported observations, plots from ORB6 were opened in Microsoft Paint and the coordinates of the "fixed" primary star and the plot scale (graphic pixels/arc second) determined. These three values—two for the primary star coordinates, and one for scale—were entered into a spread sheet for each binary along with the measured θ and ρ values for the binaries.

The graphic pixel location on each plot for each observation was calculated and a large "**+**" sign, centered on the location of the current observation, was then "penciled" in. To see how well observations matched the predicted time along the orbit for the night of observation, the time along each orbit, based on interpolated θ and ρ values from ORB6 ephemerides, was marked with a long, thin line. The observational sequence number was added to the plots in the lower left corner. Past observations that are **green +** are visual (micrometer) observations, **violet *** are photographic, while **blue** filled circles are speckle interferometry. A **red +** is Hipparcos, while a **red T** is Tycho.

Near or on the Line

The first set of 12 observations, shown below, was very near or essentially on the lines of the predicted elliptical paths.

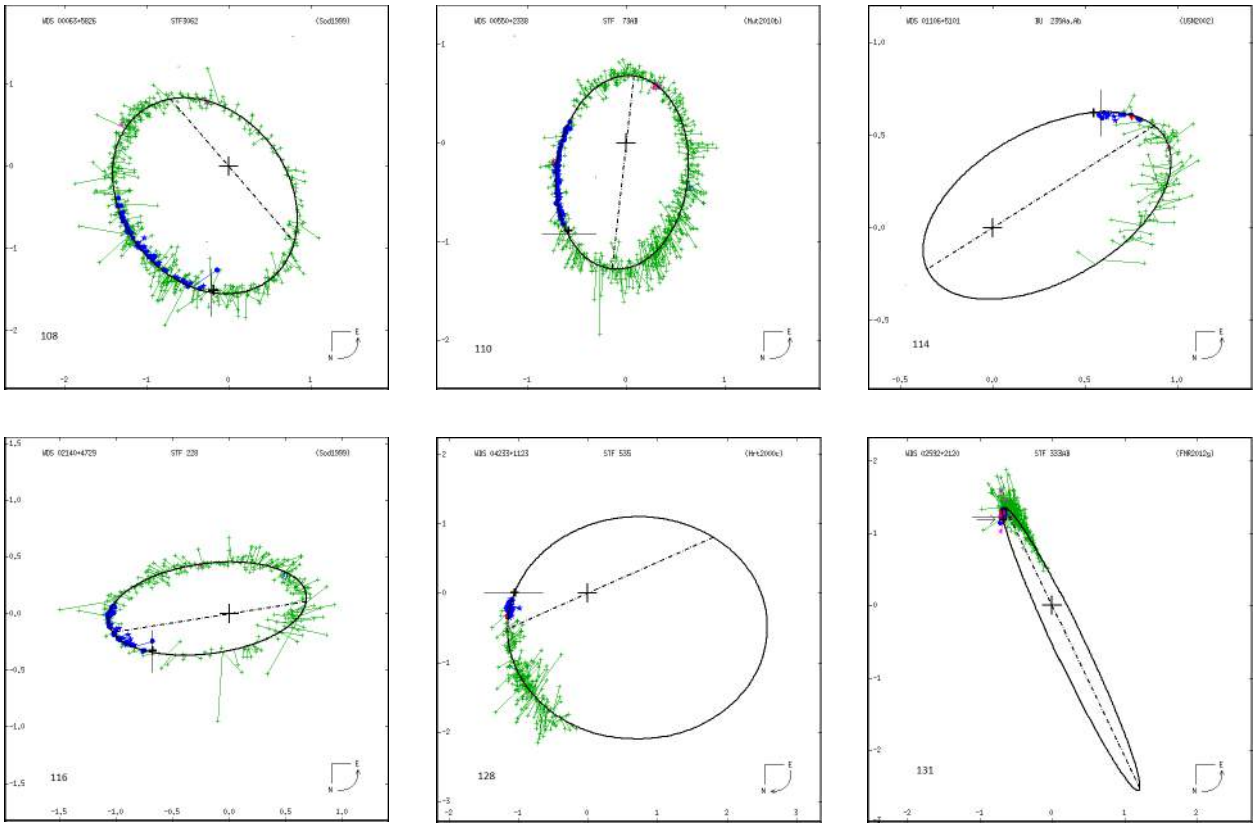

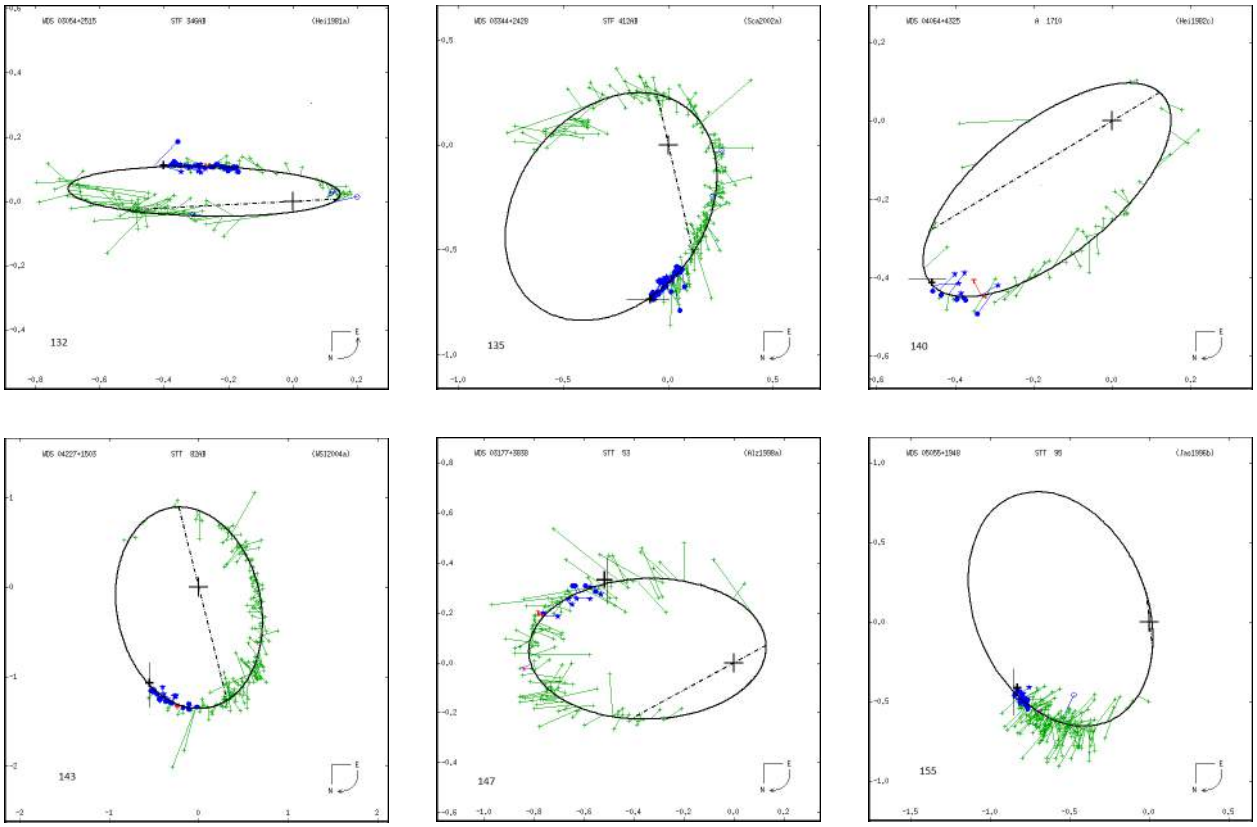

Not on the Line (but perhaps that was all right)

Although observations were not on the line for six of the 20 binaries, they were near other inteferometric measures that were also off the line (or headed off the line). This may suggest that these orbits were off and a recalculation of the orbit would have put observations on the line. Many of these orbits were just provisional (Grade 5) orbits, so it may not be worthwhile to recalculate them until further speckle interferometric observations are made. The O-C "errors" from these orbits may over-represent actual external errors.

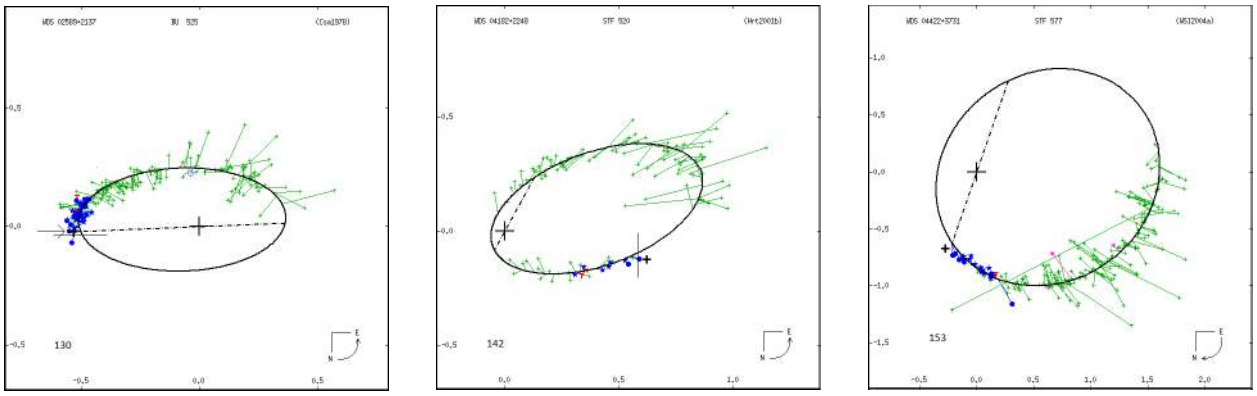

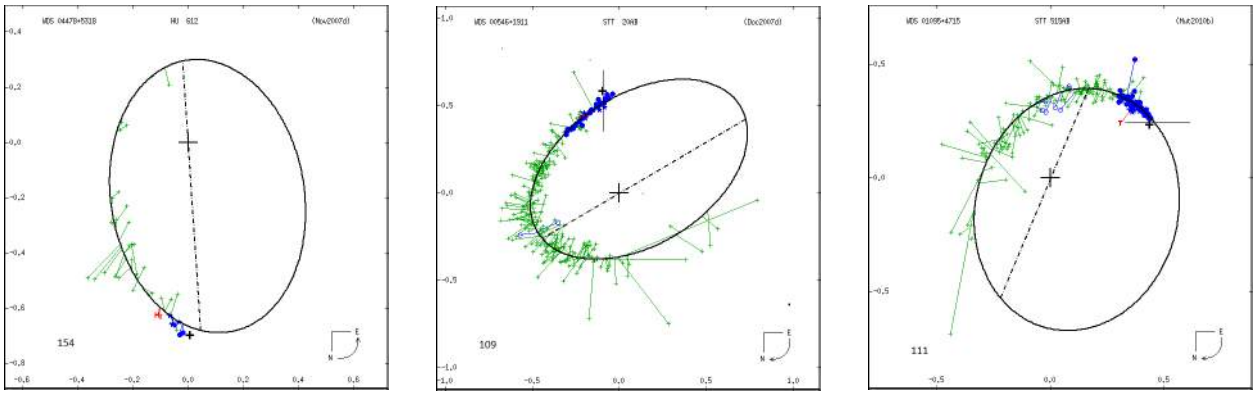

Off the Line (but not way off)

Finally, there were two cases where the plots suggested that the observations were further off than many other interferometric measurements. Perhaps such points might be expected to happen on occasion, since the 0.5-meter telescope had significantly less aperture than many of the other telescopes reporting speckle interferometry observations. Alternatively, perhaps these points are the start of a new "trend" or direction for speckle observations. This could be the case for BU 260, although STF 202 is clearly both off the orbit and also discordant with respect to other speckle observations. The autocorrelogram for STF 202 was by far the poorest of the 20 binaries, but BU 260's looked quite normal.

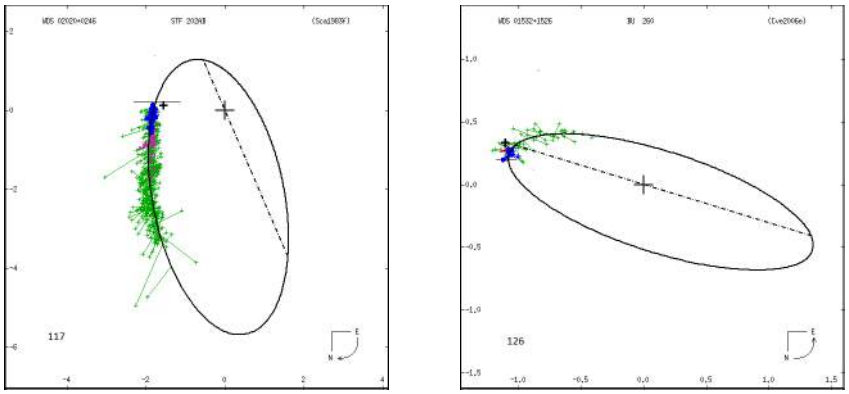

Conclusion

We measured the position angles and separations of 42 fairly close double stars over four hours with a portable speckle interferometry camera system on a 0.5-meter telescope. We reduced our data with REDUC, a program written by Florent Losse. We discovered two new triple star systems and derived orbits for the inner pairs.

Acknowledgments

We thank the American Astronomical Society for funding the Andor Luca-S EMCCD camera and also Andor for making a demonstration unit available at a reduced price. We also thank the US Naval Observatory for extensive use of the *Washington Double Star Catalog,* the *Sixth Catalog of Orbits of Visual Binary Stars,* and the *Forth Interferometric Catalog*. A special thanks goes to Brian Mason for past observations and to Robert Buchheim for help with orbital plots. Finally, we thank the reviewers of this paper for their helpful suggestions: Robert Buchheim, Joseph Carro, Jerry Foote, Thomas Frey, Jolyon Johnson, Brian Mason, Thomas Smith, Vera Wallen, and Ed Wiley.

References

Alzner, A. 1998. *A&AS*, 132, 253.

Castets, M. & Tregon, B. 2009. *El Observador de Estrellas Dobles*, 3, 7.

Costa, J. M. 1978. *Inf. Circ.*, 75.

Cvetkovic, Z. & Novakovic, B. 2006. *Ser AJ*, 173, 73.

Debehogne, H. & de Freitas Mourao, R. R. 1977. *Astronomy and Astrophysics*, 61, 453-457.

Docobo, J. A. & Ling, J. F. 2007. *AJ* 133, 1209.

Genet, R. M. 2013. *Journal of Astronomical Instrumentation*. In preparation.

Hartkopf, W. I. & Mason, B. D. 2012. *Sixth Catalog of Orbits of Visual Binary Stars,* Washington: US Naval Observatory.

Hartkopf, W. I. & Mason, B. D. 2000. *IAUC,* 142.

Hartkopf, W. I. & Mason, B. D. 2001. *IAUC,* 145.

Heintz, W. D. 1978. *Double Stars (revised edition)*. Ed. Dordrecht, D. *Geophysics and Astrophysics Monographs*, 15.

Heintz, W. D. 1982. *IAUC,* 88.

Heintz, W. D. 1997. *ApJS* 111, 335.

Irwin A. W., Yang S. L. S., & Walker G. A. H. 1996. *PASP*, 108, 580.

Jasinta, D. M. D. 1996. *A&AS*, 118, 381.

Kiyaeva, O. V., Kisselev, A. A., Polyakov, E. V., & Rafal'Skii, V. B. 2001. Pisma Astron. *Zhur*, 27, 456.

Losse, F. 2012. REDUC V4.7. http://www.astrosurf.com/hfosaf/Reduc/Tutorial.htm

Mason, B. D., Hartkopf, W. I., Wycoff, G. L., Pascu, D., Urban, S. E., & Hall, D. M. 2004. *AJ,* 127, 539.

Mason, B. D., Wycoff, G. L., & Hartkopf, W. I. 2012a. *The Washington Double Star Catalog,* Washington: US Naval Observatory.

Mason, B. D., Henry, T. J., Soderblom. D. R., Hartkopf, W. I., Holdenreid, E. R., Rafferty, T. J., & Urban, S. E. 2012b. In preparation.

McAlister, H. A., Hartkopf, W. I., Hutter, D. J., & Franz, O. G. 1987. *AJ,* 93, 688.

Mendenhall, W., Wackerly, D. D., & Shara, M. M., 1990. *Mathematical Statistics with Applications,* 4. Boston: PWS-Kent.

Muterspaugh, M. W., Hartkopf, W. I., Lane, B. F., O'Connell, J., Williamson, M., Kulkarni, S. R., Konacki, M., Burke, B. F., Colavita, M. M., Shao, M., & Wiktorowicz, S. J. 2010. *AJ,* 140, 1623.

Novakovic, B. 2007. *ChJAA*, 7, 415.

Prieur, J. L., Scardia, M., Pansecchi, L., Argyle, R. W., Sala, M., Ghigo, M., Koechlin, L., & Aristidi, E. 2008. *MNRAS*, 387, 772.

Rica, F. M., Barrena, R., Vazquez, G., Henriquez, J. A., & Hernandez, F. 2012. *MNRAS*, 419, 197.

Scardia, M., Prieur, J. L., Koechlin, L., & Aristidi, E. 2002. *IAUC*, 147.

Scardia, M., Prieur, J. L., Pansecchi, L., Argyle, R. W., & Sala, M. 2011. *AN*, 332, 508.

Scardia, M., Prieur, J. L., Pansecchi, L., Argyle, R. W., Basso, S., Sala, M., Ghigo, M., Koechlin, L., & Aristidi, E. 2007. *MNRAS*, 374, 965.

Schmidt-Kaler, T. H. 1982. Physical parameters of the stars. In *Landolt-Bornstein New Series*, 2b, astronomy and astrophysics – stars and star cluster. Eds. Schaifers, K. & Voigt, H. H. New York: Springer.

Seymour, D., Mason, B. D., Hartkopf, W. I., & Wycoff, G. L. 2002. *AJ,* 123, 1023.

Soderhjelm, S. 1999. *A&A*, 341, 121.

van den Bos, W. H. 1926. *CiUO*, 68, 352.

Van Leeuwen, F. 2007. *Hipparcos, the New Reduction of the Raw Data*. Astrophysics & Space Science Library. Berlin: Springer, 350.